Materials Science-Poland, 31(2), 2013, pp. 264-268
http://www.materialsscience.pwr.wroc.pl/
DOI: 10.2478/s13536-012-0100-6

VERSITA

Synthesis of maghemite (γ-Fe_2O_3) nanoparticles by thermal-decomposition of magnetite (Fe_3O_4) nanoparticles

M. ALIAHMAD*, N. NASIRI MOGHADDAM

Physics Department, Faculty of Science, University of Sistan and Baluchestan, P. O. Box 98135-674, Zahedan, Iran.

In this research work, we prepared γ-Fe_2O_3 nanoparticles by thermal-decomposition of Fe_3O_4. The Fe_3O_4 nanoparticles were synthesized via co-precipitation method at room temperature. This simple, soft and cheap method is suitable for preparation of iron oxide nanoparticles (γ-Fe_2O_3; Fe_3O_4). The samples were characterized by X-ray diffraction (XRD), Fourier transform infrared spectroscopy (FT-IR), transmission electron microscopy (TEM), vibrating sample magnetometer and differential scanning calorimeter (DSC). The XRD and FT-IR results indicated the formation of γ-Fe_2O_3 and Fe_3O_4 nanoparticles. The TEM images showed that the γ-Fe_2O_3 and Fe_3O_4 were spherical, and their size was 18 and 22 nm respectively. Magnetic properties have been measured by VSM at room temperature. Hysteresis loops showed that the γ-Fe_2O_3 and Fe_3O_4 nanoparticles were super-paramagnetic.

Keywords: *co-precipitation; super-paramagnetic nanoparticles; maghemite; magnetite*

1. Introduction

Recently, nanoparticles have attracted interest of scientists in various areas of biomedical research because of their unique properties. It is already known that one of the major breakthroughs in the application of nanoparticles is the realization of the steric stabilization which can increase the particle stability in the biological environment and provide application opportunities of nanoparticles in drug delivery systems for achieving drug targeting and controlled drug release [1]. Among these particles, magnetic nanoparticles have attracted much interest not only in the field of magnetic recording but also in areas of medical care and magnetic sensing. Especially, nanoparticles of iron oxide such as Fe_3O_4 and γ-Fe_2O_3 have been reported to be applicable as a material for the use in drug delivery systems (DDS), magnetic resonance imaging (MRI), and cancer therapy [2–4]. However, these applications are still subject to many constraints, for instance, particle size, monodispersity, magnetization, stability, non-toxicity, biocompatibility, injectability, and short blood half-life of magnetic nanoparticles for in vivo applications. Among them, size control is a critical parameter that controls both physicochemical and pharmacokinetic properties. In fact, synthesis of respective nanoparticles with controllable size and size distribution remains a great challenge, particularly in the aspect of small sizes [5]. In magnetic nanoparticles, energy barrier against magnetization reversal is comparable to thermal activation effects resulting in their superparamagnetic behavior with negligible coercivity and the lack of magnetization saturation [6]. Many ways to prepare Fe_3O_4 and γ-Fe_2O_3 nanoparticles, such as arc-discharge, mechanical grinding, laser ablation, microemulsions, co-precipitation, sol-gel and high temperature decomposition of organic precursors, etc, have been reported. These methods are suitable for preparation magnetite and maghemite with different controllable particle diameters. However, preparation of well-dispersed aqueous Fe_3O_4 nanoparticles has met with very limited success [6, 7].

In this study, a modified co-precipitation synthesis of divalent/trivalent iron salts using aqueous ammonium hydroxide ($NH_3{\cdot}H_2O$) was used to produce super-paramagnetic Fe_3O_4 and γ-Fe_2O_3 nanoparticles, which were well-dispersed in an

*E-mail: aliahmad@phys.usb.ac.ir

aqueous solution. In the drying process, nitrogen was used to protect divalent iron salts from oxidation. After 2 hour calcination at 300 °C in these conditions, the Fe_3O_4 nanoparticles transformed into brown γ-Fe_2O_3.

The preparation of magnetite nanoparticles by using co-precipitation approach is expected to give homogeneous and phase-pure specimens with a narrow size distribution of particles. The advantage of thermal-decomposition under nitrogen atmosphere for producing the maghemite nanoparticles is low sintering temperature and possibility of obtaining pure crystalline phase.

2. Materials and methods

In present study, two kinds of samples were synthesized in different processes. The reagents used for the synthesis included: ferric chloride hexa-hydrate ($FeCl_3{\cdot}6H_2O$), ferrous chloride tetrahydrate ($FeCl_2{\cdot}4H_2O$), deionized water, ethanol, and ammonium hydroxide (NH_4OH, 25 % of ammonia).

The sample of Fe_3O_4 was synthesized by the co-precipitation method. 300 ml of deionized water was deoxygenated by bubbling N_2 gas for 30 min in a 500 ml flask. Subsequently, ammonium hydroxide (1 M) was added and the mixture was stirred magnetically for 10 min under a nitrogen atmosphere. Afterwards, ferrous chloride 0.5 M and ferric chloride 0.5 M were added and then the residual was aged for 10 min before being separated. Below a possible reaction for the formation of Fe_3O_4 particle is presented:

$$Fe^{2+} + 2Fe^{3+} + 8NH_3 \cdot H_2O \rightarrow \\ \rightarrow Fe_3O_4 + 8NH_4^+ + 4H_2O \qquad (1)$$

Finally, the Fe_3O_4 product was separated by a centrifugal pump and washed twice with deionized water and ethanol. The obtained fine Fe_3O_4 powders were dried at 60 °C for 8 hours.

In case of γ-Fe_2O_3, the magnetite nanoparticles were calcined at 300 °C. The particles were kept at this temperature for 2 hours in a muffle furnace to obtain the light brown γ-Fe_2O_3 nanoparticles.

3. Results and discussion

3.1. X-ray diffraction

The crystalline structure of these nanoparticles was characterized by X-ray diffraction (XRD, PHILIPS, XPert-MPD) using CuKα (λ = 0.154 nm) radiation within a range of 10 – 70° at a rate of 2°/min.

XRD measurement results for magnetite and maghemite nanoparticles are shown in Figs. 1a and 1b. All diffraction peaks in Fig. 1a are consistent with the standard structure of magnetite (JCPDS card No. 74-0748) and diffraction peaks in Fig. 1b are consistent with the standard structure of maghemite (JCPDS card No. 39-1346). The average crystallite sizes of magnetite and maghemite are about 12 and 14 nm, respectively. The average crystallite sizes in the samples were calculated from the XRD line broadening using the Scherrer's formula:

$$d_{hkl} = \frac{0.9\lambda}{\beta \cos\theta} \qquad (2)$$

where, d is the crystallite size (nm), θ is the angle of incidence, λ is the wavelength of X-ray diffraction (λ = 0.15406 nm), β is the full width at half maximum [8].

The XRD patterns confirm crystallinity of Fe_3O_4 and γ -Fe_2O_3 nanoparticles very well.

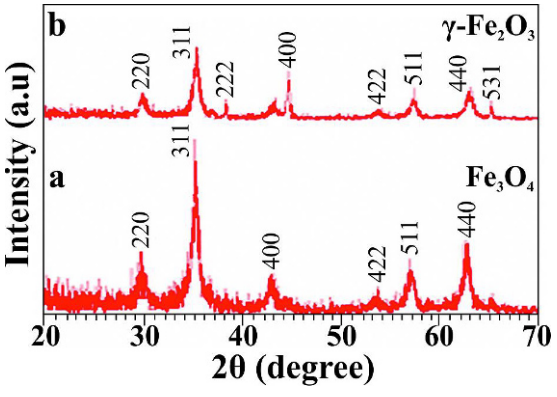

Fig. 1. XRD patterns of Fe_3O_4 (a) and γ-Fe_2O_3 (b).

3.2. FT-IR Spectra

FT-IR spectra were measured in a transmission mode on a spectrophotometer (Model RT-

DLATGS) under ambient conditions in a range of 400 to 4000 cm^{-1} with a spectral resolution of 4 cm^{-1} in the transmittance mode. Fourier transform infrared spectrometer was employed to analyze the surface characteristics of the nanoparticles.

To confirm the structure of the samples FT-IR spectrum was recorded at room temperature. In Fig. 2a strong absorption band at 586 cm^{-1} is assigned to vibration of the Fe–O functional groups. Two peaks at about 2360 and 3424 cm^{-1} can be assigned to CO_2 and H_2O respectively [9, 10].

The FT-IR analysis revealed that the Fe_3O_4 nanocrystals are free of organic contaminants. In Fig. 2b absorption band at 562 cm^{-1} can be assigned to vibration of the Fe–O functional group. Two peaks at about 3420 cm^{-1} and 2361 cm^{-1} come from the hydroxyl group (OH^-) and CO_2 present in the atmosphere. The peak at 1630 cm^{-1} is related to the hydroxide group [10, 11]. These nanoparticles are free from organic contaminants, too.

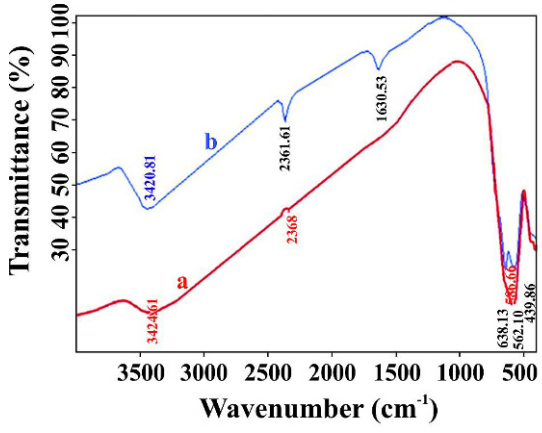

Fig. 2. FT-IR spectra of (a) Fe_3O_4 and γ-Fe_2O_3 (b).

3.3. TEM images

The morphology and average particle size were investigated with transmission electron microscope (TEM PHILIPS CM20). The size distribution was determined with a particle size analyzer (ZETASIZER, MALVERN Nano-ZS90).

Figs. 3a and 3b show the TEM images of Fe_3O_4 and γ-Fe_2O_3 nanoparticles, respectively. The TEM images confirm the spherical morphology and narrow size distribution of Fe_3O_4 and γ-Fe_2O_3 nanoparticles. The average size of nanoparticles is 18 and 22 nm for magnetite and maghemite nanoparticles, respectively.

This shows a difference between the particle size and crystallite size obtained using Scherrer's formula.

3.4. Vibrating sample magnetometer (VSM) measurements

A vibrating sample magnetometer (VSM) was used to measure magnetic properties of the samples at room temperature.

Fig. 4 displays the magnetization curves of samples Fe_3O_4 and γ-Fe_2O_3 at room temperature. The two samples show super-paramagnetic behavior with zero coercivity and remanence. The shape of the hysteresis loop is depended on particle size. When the particle size decreases, the number of magnetic domains per particle decreases down to the limit where it is energetically unfavorable for a domain wall to exist. Below a critical diameter, the magnetic particles have a single domain; the particles are then super-paramagnetic. The super-paramagnetic nanoparticles fluctuate due to thermal energy, this fluctuation tends to randomize the moments of the nanoparticles unless a magnetic field is applied, at this condition coercivity is negligible [12]. This is related to the fine crystallite sizes of Fe_3O_4 and γ-Fe_2O_3 particles, which are in the range of 20 – 50 nm [13]. The values of saturation magnetization (Ms) of Fe_3O_4 and γ-Fe_2O_3 are 45 and 31 emu/g, respectively, and are lower than that of the bulk Fe_3O_4 (92 emu/g) and γ-Fe_2O_3 (73.5 emu/g) [11, 14].

No magnetization saturation is observed in the range of the applied magnetic fields, confirming super-paramagnetic behavior of the particles.

3.5. Differential scanning calorimeter (DSC) measurements

Thermal properties were studied with a differential scanning calorimeter (DSC) using STA409PG model. The measurements were conducted at a heating rate of 10 °C/min in a dynamic

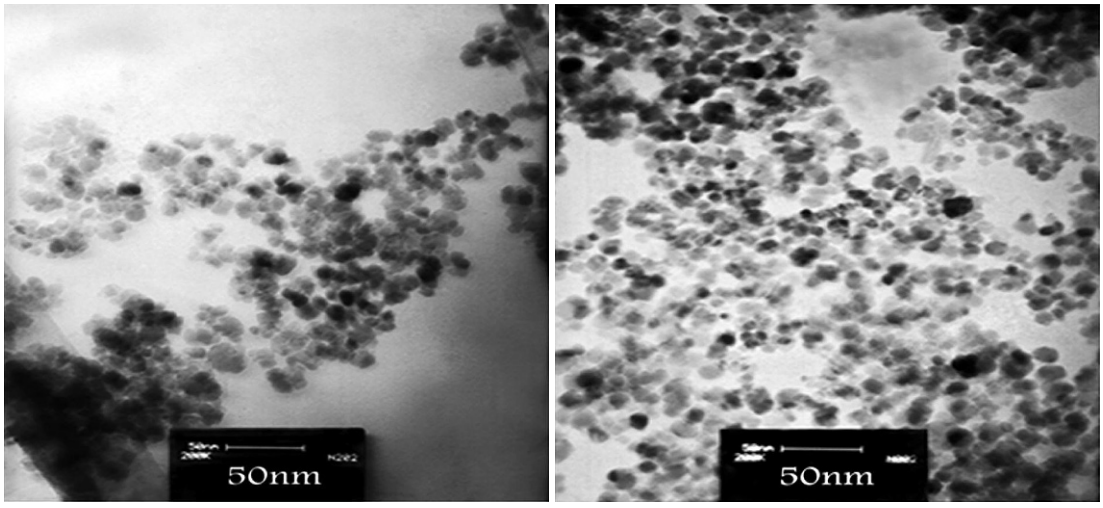

(a) (b)

Fig. 3. TEM images of Fe_3O_4 (a) and γ-Fe_2O_3 (b) nanoparticles.

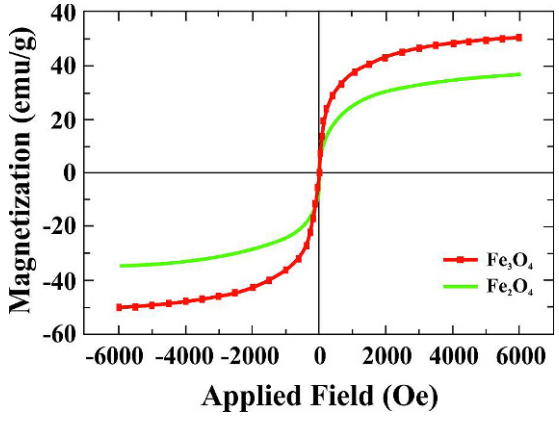

Fig. 4. Magnetization curve of Fe_3O_4 (a) and γ-Fe_2O_3 (b).

argon atmosphere. Thermo-gravimetric (TG) and differential scanning calorimeter (DSC) results for the magnetite and maghemite nanoparticles are shown in Fig. 5. Fig. 5a shows the results of the analysis for magnetite nanoparticles. The weight loss at the temperatures ranging from 35 °C to about 100 °C and from 320 °C to 360 °C is due to desorption of physically and chemically adsorbed water, respectively. There is an endothermic peak at 270 °C. No weight loss is observed in this area. According to the mass conservation, this peak corresponds to the transformation of Fe_3O_4 into γ-Fe_2O_3 [11, 15–17]. Two exothermic peaks at 480 °C and 540 °C correspond to phase change. It seems that these peaks are related to formation of ε-Fe_2O_3 and α-Fe_2O_3 phase, respectively [18]. The weight loss in the temperature range of 700 °C to 900 °C is related to α-Fe_2O_3 nanoparticles.

Fig. 5b shows the results of analysis of maghemite nanoparticles. The two exothermic peaks at 480 °C and 540 °C correspond to decomposition of γ-Fe_2O_3 to ε-Fe_2O_3 and α-Fe_2O_3 respectively. The weight loss of 2 % and 5 % from 90 – 300 °C and 700 – 900 °C is the result of physical loss of water and the weight loss of α-Fe_2O_3, respectively.

4. Conclusions

Spherical, high purity Fe_3O_4 nanoparticles have been prepared by controlled chemical co-precipitation method. The γ-Fe_2O_3 nanoparticles were produced by thermal-decomposition of Fe_3O_4 at 300 °C for 2 hour duration. The mean particle size of magnetite and maghemite nanoparticles determined from TEM images was 18 and 22 nm, respectively. The magnetization of magnetite nanoparticles at room temperature was 45 emu/g at the magnetic field of 3000 Oe. For the maghemite nanoparticles, the magnetization saturation was 31 emu/g at the field of 2000 Oe. Due to small mean size, the obtained nanoparticles

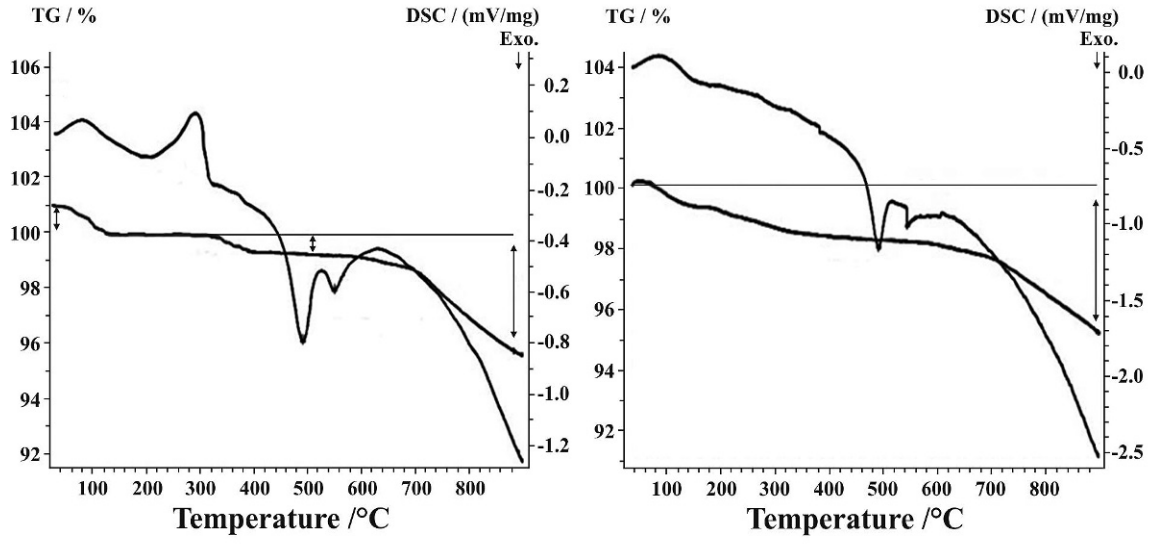

(a) (b)

Fig. 5. TG-DSC curves of Fe_3O_4 (a) and γ-Fe_2O_3 (b).

were super-paramagnetic with thermally fluctuating magnetic moments resulting in the sigmoidal, anhysteretic (Langevine-type) M-H curve. The nanoparticles which were prepared by these methods have a good potential to be applied as industrial materials. In summary, we showed that chemical co-precipitation method followed by a proper thermal treatment lead to phase pure small γ-Fe_2O_3 particles with a good crystalline structure and a narrow size distribution.

Acknowledgements

This work supported by University of Sistan and Baluchestan of Iran. The authors are grateful for the supports from the University of Sistan and Baluchestan.

References

[1] JING S., ZHOU S., HOU P., YANG Y., WENG J., LI X., LI M., *J. Biomed. Mater. Res.*, A 80 (2007), 333.
[2] WANG X., ZHANG R., WU C., DAI Y., SONG M., GUTMANN S., GAO F., LV G., LI J., LI X., GUAN Z., FU D., CHEN B., *J. Biomed. Mater. Res.*, A 80 (2007), 852.
[3] YUKSEL K., *J. Magn. Mater.*, 300 (2006), 327.
[4] IIDA H., TAKAYANAGI K., NAKANISHI T., OSAKA T., *J. Colloid Interface Sci.*, 314 (2007), 274.
[5] LING H.L., PILKO S., WU J.H., JUNG M.H., MIN J.H., LEE J.H., AN B.H., KIM Y.K., *J. Magn. Mater.*, 310 (2007), 815.
[6] LIAN S., KANG Z., WANG E., JIANG M., HU C., *Solid State Commun.*, 127(2003), 605.
[7] SADEGHI M., SARABADANI P., KARAMI H., *J. Magn. Mater.*, 283 (2010), 297.
[8] ABARESHI M., GOHARSHADI E.K., ZEBARJAD S.M., KHANDAN FADAFAN H., YUSSEFI A., *J. Magn. Mater.*, 322 (2010), 3895.
[9] SHEN Y.F., TANG J., NIE Z.H., WANG Y.D., REN Y., ZUO L., *J. Separ. Purif. Technol.*, 68 (2009), 312.
[10] DAREZERESHKI E., *J. Mater. Lett.*, 64 (2010), 1471.
[11] DAREZERESHKI E., *J. Mater. Lett.*, 65 (2010), 642.
[12] SELLMYER D., SKOMSKI R., Advanced magnetic nanostructures, Springer, New York, 2006.
[13] DUTZ S., HERGT R., *J. Nano- Electron. Phys.*, 4 (2012), 02010.
[14] ALIBEIGI S., VAEZI M.R., *J. Chem. Eng. Technol.*, 31 (2008), 1591.
[15] MODY V.V., SIWALE R., SINGH A., MODY H.R., *Adv. Powder. Technol.*, 2 (2010), 282.
[16] LAI J., SHAFI K.V.P.M., LOOS K., ULNAM A., LEE Y., VOGT T., ESTORNES C., *J. Structure. AM. Chem. Soc.*, 125 (2003), 11470.
[17] XU X.N., WOLFUS Y., SHAULOV A., YESHURUN Y., *J. App. Phys.*, 91 (2002), 4611.
[18] CORNELL R.M., SCHWERTMANN U., The iron oxides: structure, properties, reactions, occurrences. John Wiley, Cambridge, 2003.

Received 2012-12-06
Accepted 2013-02-15